[논 문] 한국재료학회지
Korean J. Mater. Res.
Vol. 29, No. 9 (2019)

https://doi.org/10.3740/MRSK.2019.29.9.525

# Lightweight and Performance of Anti-Collision Strength of Automobiles Based on Carbon Fiber Composites

Hongtao Zhang†

Henan College of Transportation, Zhengzhou, Henan 450005, China

(Received May 31, 2019 : Revised August 28, 2019 : Accepted August 30, 2019)

**Abstract** The widespread use of automobiles has greatly increased energy demand and exhaust gas pollution. In order to save energy, reduce emissions and protect the environment, making lightweights automobiles is an effective measure. In this paper, carbon fiber composites and automobile B-pillars are briefly introduced, and then the mechanical properties and impact resistance of the DC590 steel B-pillars and carbon fiber composites B-pillars are simulated by the ABAQUS finite element software. The results show that the quality of compound B-pillars is reduced by 50.76 % under the same dimensions, and the mechanical property of unit mass is significantly better than that of metal B-pillars. In the course of a collision, the kinetic energy of the two B-pillars is converted into internal energy, but the total energy remains the same; the converted internal energy of the composite B-pillars is greater, the deformation is smaller and the maximum intrusion and intrusion speed is also smaller, indicating that the anti-collision performance of the composite B-pillars is excellent. In summary, the carbon fiber composites can not only reduce the quality of the B-pillars, but also improve their anti-collision performance..

**Key words** carbon fiber, lightweight, anti-collision performance, automobile B-pillar.

## 1. Introduction

With the rapid development of the economy, the cars used by individuals have been becoming more and more popular. Although the popularity of automobiles has facilitated people's travel, it also brings about the problem of increasing energy consumption and exhaust pollution.[1] Gasoline is used as the main energy source for Traditional automobiles. Although there are hybrids of electricity and oil and electricity, the mainstream is still fossil energy. Therefore, in addition to the large amount of carbon dioxide generated, there will be atmospheric pollutants such as sulfur dioxide, nitrogen dioxide and particulate floats during the operation of the automobiles.[2] In order to reduce the air pollution caused by the operation of automobiles, the cars need to be improved. There are two directions for improvement,[3] one is to improve the utilization of fuel of the engine to obtain a longer lasting output with less fuel, and the other is to reduce the own weight of the automobiles to improve the utilization of fuel. In comparison between the two methods, the former method solves the problem fundamentally, but the required cycle is too long, while the latter is simple and clear, and the implementation difficulty is relatively low. At the same time, reducing the weight of the automobile can also improve the operating performance of the automobile. The lightweight of the own weight of the vehicle is not simply to reduce parts or reduce the amount of materials, but to use lightweight materials under the premise of ensuring or even exceeding the strength of the original structure and to optimize the structure, so as to achieve the purpose of reducing the weight of the body.[4] Zhao et al.[5] proposed a method of structural design and optimization of the front bumper system using carbon fiber composites. Through the actual vehicle test, the optimized bumper system reduced the weight by 31.5 % while meeting the requirements of strength and crash resistance. Kim et al.[6] replaced the glass mat thermoplastic (GMT) with glass/carbon mat thermoplastic (GCMT) to reduce the weight of the car bumper. The simulation experiments showed that the optimized design of the GCMT bumper is 33 % lighter than the traditional GMT bumper with better impact performance. Yu et al.[7] used carbon fiber reinforced

†Corresponding author
E-Mail : hongtzhtao@126.com (Hongtao Zhang, Henan College of Transportation)

plastic bumpers instead of traditional high-strength steel bumpers and simulated the two bumpers. The results showed that the carbon fiber reinforced plastic bumper beams had better performance of energy absorption and characteristics of dynamic response than steel bumper beams, whose weight was significantly reduced by nearly 50 %. In this paper, the carbon fiber composites and the automobile B-pillars are briefly introduced, and then the mechanical properties and impact resistance of the DC590 steel B-pillars and carbon fiber composites B-pillars are simulated by the ABAQUS finite element software.

## 2. Carbon Fiber Composites

Composites are man-made materials composed of two or more different materials of different chemical or physical properties, including reinforced concrete, foam sandwich panels, etc. In this paper, the carbon fiber composite[8] is selected, and its basic structure is shown in Fig. 1, which can be divided into three models: parallel, series and shear. The three models can be used to calculate the basic elastic mechanics parameters of carbon fiber composites. The fiber-to-elastic modulus is calculated firstly by using the simplified parallel model of the composites. The connection between the matrix and the fiber is set as an adhesive connection, which is ideal for full bonding, ensuring that the matrix and the fiber have the same deformation under the same load, thus the strains of the matrix, fiber and composites are the same, i.e.,

$$\varepsilon_1 = \varepsilon_f = \varepsilon_m , \tag{1}$$

where $\varepsilon_1, \varepsilon_f, \varepsilon_m$ represent the strain of the whole, fiber and matrix respectively. The longitudinal load on the parallel model is expressed as $P_1$,

$$P_1 = P_m + P_f , \tag{2}$$

where $P_m, P_f$ respectively indicate the load on the matrix and fiber. According to the principle that the load on the section is the product of the section stress and the cross-sectional area and based on equation (1), the formula can be obtained[9]:

$$\frac{\sigma_1 A_1}{\varepsilon_1} = \frac{\sigma_m A_m}{\varepsilon_m} + \frac{\sigma_f A_f}{\varepsilon_f} , \tag{3}$$

where $\sigma_1, \sigma_f, \sigma_m$ respectively represent the stresses of the whole, fiber and matrix, and $A_1, A_f, A_m$ respectively represent the cross-sectional area of the whole, fiber and matrix. The modulus of elasticity is defined as the ratio of stress to strain, dividing the equations on both sides of equation (3) by $A_1$. Because the material distribution in the parallel model is uniform, the ratio of the cross-sectional area is equivalent to the volume fraction ratio, then the formula can be derived:

$$\begin{cases} E_1 = E_m V_m + E_f V_f \\ V_m + V_f = 1 \end{cases} , \tag{4}$$

where $E_1, E_f, E_m$ respectively represent the modulus of elasticity of the whole, the fiber and the matrix, and $V_f, V_m$ respectively represent the volume ratio of the fiber and the matrix. Then according to the similar method described above, the transverse elastic modulus and in-plane shear modulus of the carbon fiber composites are initially calculated by using the tandem model and the shear model, and the formula after derivation is integrated[10]:

$$\begin{cases} E_1 = E_m V_m + E_f V_f \\ E_2 = \dfrac{E_f E_m}{E_m V_f + E_f V_m} \\ G = \dfrac{G_f G_m}{G_m V_f + G_f V_m} \\ V_m + V_f = 1 \end{cases} , \tag{5}$$

where $E_1, E_2, G$ respectively represent the fiber orientation, transverse elastic modulus and in-plane shear modulus of the whole, and $G_f, G_m$ respectively represent the shear modulus of the fiber and matrix. The formula derived above reflects that the mechanical properties of carbon fiber composites depend not only on the mechanical properties of the matrix and fiber, but also on the proportion of the two materials in the overall structure. The structural model in Fig. 1 belongs to the simplified

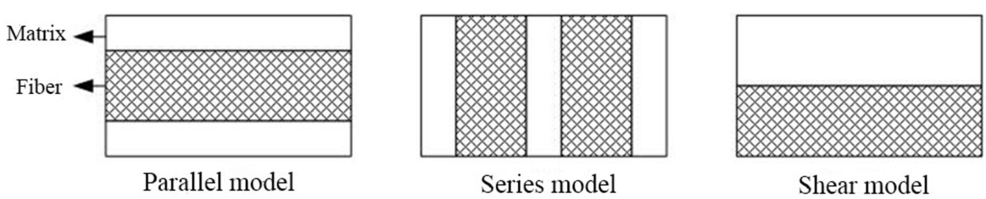


**Fig. 1.** Basic structure of carbon fiber composites.

ideal model. In the subsequent formula derivation, the deformations produced by the two materials of different properties are also treated as the same. In addition, as a complex material, the mechanical properties are affected by various different factors, so experiments are needed to obtain accurate mechanical parameters in the practical application. However, the formula based on the ideal model has a good reference value in the preliminary design of the structure.

## 3. The Automobile B-pillars

Fig. 2 is a schematic diagram of the basic structure of ordinary automobile, which is used for indicating the position of B-pillar and is not a newly designed automobile structure. Automobile B-pillars[11] are the two pillars at the seat belt of the driver's seat in the entire car frame. In addition, the pillars on both sides of the front windshield of the driver's seat are A-pillars, and the pillars on both sides of the rear windshield are C-pillars. The car frame, which excludes all parts of the car, is called the white body, acting to stabilize the overall structure and provide a platform for integrating the car parts. In addition to dividing the boundary of the door frame, the A, B and C pillars in the white body also plays a supporting role in the rolling and collision of the vehicle. Therefore, the strength of the three pillars is very important for the car. Since the B-pillar is located between the front door and the rear door, the B-pillar is simultaneously subjected to the pressure of the roof and the front and rear doors. During the operation of the car, the load on the car is transmitted to the white body through the tire and suspension system. The lateral force transmitted to the B-pillar is relatively small, so which is ignored in this paper; the longitudinal and vertical loads are transmitted to the entire body, and the B-pillar plays a role in strengthening the stability of the entire structure of the white body. In addition to its own load, when the side of the vehicle is impacted, the B-pillar is the only structure capable of carrying the impact load, whose strength is directly related to the safety of the personnel inside the vehicle.

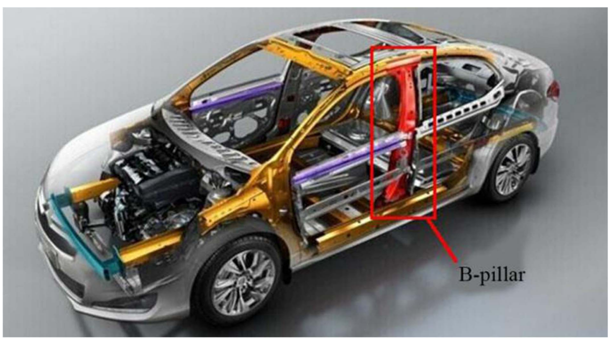


**Fig. 2.** The automobile B-pillar.

The mechanical properties of the B-pillars of the car body-in-white are very important for stabilizing the body structure and resisting side impact. The commonly used material is high-strength steel. Although the high-strength steel can meet the stability of the car body and the effect of anti-side impact, the high-strength steel is metal with large mass, which will increase the weight of the car body to some extent and the burden of the B-pillars[12]. The emergence of carbon fiber composites solves this problem, because of their mechanical properties that are not worse than metals and are lighter in weight. The process of designing the B-pillars using the carbon fiber composites is shown in Fig. 3. Firstly, the model is drawn according to the structure of the original high-strength steel B-pillars; secondly, the model is divided according to a certain ratio to facilitate the subsequent model simplification and reduce the difficulty of material replacement; then the unnecessary chamfers and screw holes are removed to simplify the model after the model is divided; and finally the metal material in the model is replaced with the carbon fiber composites by using the theory of the equal stiffness approximation. Because the density between the two materials is different, under the premise of ensuring the same stiffness, the dimensions before and after replacement must be different. The calculation formula[13] is:

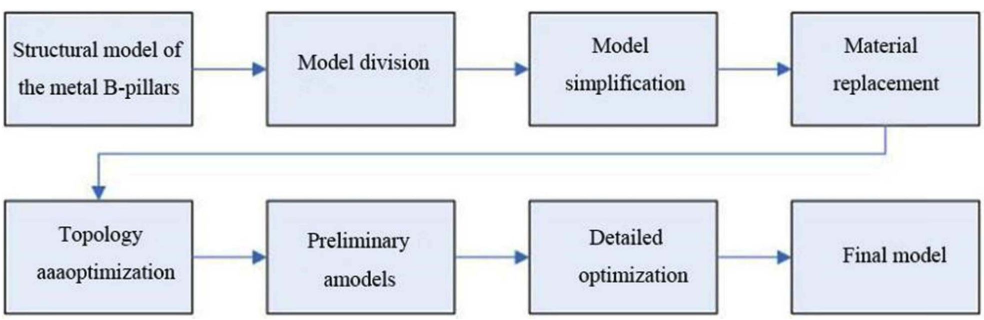


**Fig. 3.** Design flow of the carbon fiber composites B-pillars.

$$\begin{cases} E_M I_M = E_C I_C \\ I_M = \dfrac{b_M h_M^3}{12} \\ I_M = \dfrac{b_C h_C^3}{12} \end{cases}, \tag{6}$$

where $E_M, E_C$ respectively represent the elastic modulus of the original metal and composites, $I_M, I_C$ respectively represent the inertia moment of the cross-section of the original metal and composites, $b_M, b_C$ respectively represent the width of the cross-section of the original metal and composites, and $h_M, h_C$ respectively represent the thickness of the cross-section of the original metal and composites. The following formula can be obtained after converting equation (6):

$$\frac{d_M}{d_C} = \left(\frac{E_C}{E_M}\right)^{\frac{1}{\theta}}, \tag{7}$$

where $d_M, d_C$ respectively represent the thickness of the original metal and composites, and $\theta$ is a constant usually between 1 and 3. After the material of B-pillars is replaced, the topology is optimized, and the preliminary model is obtained by removing or replenishing the defects of the model whose material is replaced. The preliminary model is only a model blank having a general shape of the B-pillars, which cannot be directly used for production, so detailed optimization on the model blank is needed according to the requirements to obtain the final model.

## 4. Simulation Analysis (Analysis of mechanical properties and collision of lightweight)

### 4.1 Experimental environment

In this paper, the metal B-pillars and carbon fiber composites B-pillars are simulated by the ABAQUS finite element software.[14] The experiment is performed on a lab server with configuration of Windows 7 system, I7 processor and 16 GB memory.

### 4.2 Model parameters

The B-pillar model of this study refers to the structure of H-shaped arch shown in Fig. 2. In order to facilitate the calculation, the structure of the automobile B-pillars is simplified and idealized, as shown in Fig. 4, which is a H-shaped long beam column. The section of the long beam in the middle is trapezoid; the length of the bottom surface of the H-shaped beam column is 600 mm; the length of the top surface is 580 mm. The length and width of bottom surface A are 45 mm and 25 mm respectively. The length and width of top surface A are 40 mm and 20 mm respectively. The length and width of bottom surface C are 70 mm and 40 mm respectively. The length and width of top surface C are 65 mm and 35 mm respectively.

2×2 mm grid is used in grid division on the B-pillars model, and there are totally 11,348 cell grids. The metal B-pillars is made of DC590 steel, and its mechanical parameters are as follows: the density is 7.85 g/cm, the Poisson ratio is 0.30, the elastic modulus is 210 GPa, and the yield strength is 418 MPa.

As shown in Table 1, taking the parallel model in Fig. 1 as an example, one side is the first layer of the matrix, two sides are the fiber layer, and three sides are the second layer of the matrix. Compared with the high-strength steel, the mechanical properties of the composites used in this paper are more complex, so the construction of composites B-pillars cannot directly give the same mechanical parameters to all elements as the metal B-pillars. In this paper, the method of classical layering of (0°, 45°, 90°, -45°) is used 15) to lay the B-pillars with a

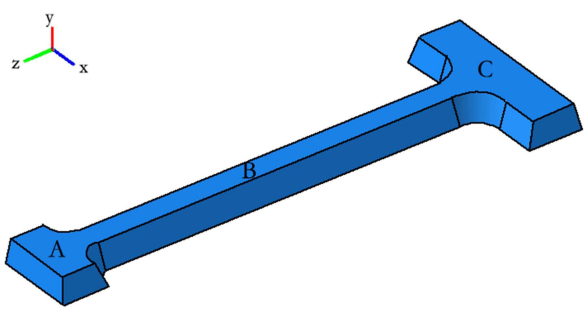

**Fig. 4.** Simplified model of the B-pillars finite element.

**Table 1.** Mechanical properties of resin-based carbon fiber composites.

| Material parameters | Numerical value | Material parameters | Numerical value |
|---|---|---|---|
| Longitudinal elastic modulus | 165 GPa | Transverse tensile strength | 40 MPa |
| Transverse modulus of elasticity | 13 GPa | Longitudinal compression strength | 1495 MPa |
| Shear modulus of 12-sided | 4.5 GPa | Lateral compressive strength | 250 MPa |
| Shear modulus of 23-sided | 2.5 GPa | Longitudinal shear strength | 68 MPa |
| Poisson's ratio | 0.31 | Transverse shear strength | 90 MPa |
| Longitudinal tensile strength | 1495 MPa | Density | 1.4 g/cm$^3$ |

thickness of 0.25 mm per layer. The thickness of the composites B-pillars is calculated by the metal B-pillars and the theory of equivalent stiffness approximation.

### 4.3 Experimental projects

The main points of force application are point A, B and C in Fig. 4, where A and C are the two horizontal transverse ends of the H-shaped beam connected with the vehicle body and B is the middle point of the long beam in the middle. The reason why the middle point of the long beam is selected as the main force bearing point is that A and C play the role of fixation, B is the main force bearing point when the vehicle is hit laterally, whose main function is to protect user, and point B is at the same level of the vital part of human body.

(1) Tensile test: the lower joint at C in the B-pillars is fixed with other parts of the vehicle body by the tie command, then a tensile load of 1 mm/s in the Z-axis direction is applied at A, and the tensile stiffness and ultimate load of the two B-pillars are calculated.

(2) Cantilever bending test: the lower joint at C in the B-pillars is fixed with other parts of the vehicle body by the tie command, then a horizontal load of 1 mm/s in the X-axis direction is applied at A, and the cantilever bending stiffness and cantilever bending ultimate load of the two B-pillars are calculated.

Fixing bending test: the upper and lower joints at A and C in the B-pillars is fixed with other parts of the vehicle body by the tie command, and then a load of 1 mm/s in the Y-axis direction is applied at B by the cylindrical rigid body. The contact between the cylindrical rigid body and the B-pillars is defined as a hard contact, and the fixed-branch bending stiffness and fixed-branch bending ultimate load of the two B-pillars are calculated.

Collision test: the upper and lower joints at the A and C in the B-pillars are fixed with other parts of the vehicle body by the tie command, and then the rigid moving column is used to hit B with a speed of 7 km/h. The impact contact is set as the contact between face and face, the contact time is set as 120 ms, and the diameter, length and mass of the moving column are100 mm, 250 mm and 250 kg respectively. The internal energy and deformation values of the impact are calculated.

### 4.4 Experimental results

After the corresponding mechanical properties are calculated by the tensile, cantilever bending and solid bending simulation experiments, it is found that the B-pillars made of carbon fiber composites are reduced by 50.76 % in mass, but different stiffness decreases, the load increases, and due to the different quality, the mechanical properties between the two B-pillars are difficult to compare. Therefore, the stiffness and ultimate load under unit mass are used to measure the effect of reducing the mass while satisfying the stiffness and load. As shown in Table 2, it can be seen that the unit mass mechanical properties of carbon fiber composites are significantly higher than that of DC590 steel, indicating that carbon fiber composites can achieve the same mechanical properties as DC590 steel with lighter weight.

For the B-pillars of automobiles, after the collision, the kinetic energy is first generated, and then the kinetic energy is absorbed and converted into internal energy, thereby reducing the kinetic energy and the deformation displacement of the B-pillars. Therefore, the variation of internal energy of the two B-pillars in Fig. 5 in the course of the collision can reflect the absorption capacity of the B-pillars for collision energy. As shown in Fig. 5, for the two B-pillars, the kinetic energy decreases during the course of the collision, and the internal energy increases, but the total energy remains constant at 1,000 J, i.e., the energy is conserved. The maximum internal energy absorbed by the metal B-pillars is 870 J, and the maximum internal energy absorbed by the carbon fiber composites B-pillars is 910 J. It can be seen that the carbon fiber composites can absorb more impact energy. In terms of the speed of kinetic energy decline and internal energy increase, the metal B-pillars is relatively faster to reach the peak of internal energy and the valley value of kinetic energy, indicating that the metal B-pillars has a faster speed of deformation and a greater degree of overall deformation when subjected to impact. In the perspective of impact resistance, the carbon fiber composites B-pillars are better.

**Table 2.** Comparison of mechanical properties of mass and unit mass between the two B-pillars.

| | DC590 steel | Carbon fiber composites | Performance improvement/% |
|---|---|---|---|
| Tensile stiffness mm/(kN · kg) | 9.65 | 12.19 | 26.21 |
| Tensile ultimate load N/kg | 22.74 | 48.87 | 114.88 |
| Cantilever bending stiffness mm/(kN · kg) | 0.04 | 0.06 | 47.13 |
| Cantilever bending ultimate load N/kg | 0.82 | 1.89 | 131.10 |
| Solid bending stiffness mm/(kN · kg) | 0.69 | 1.00 | 45.49 |
| Fixed bending ultimate load N/kg | 2.95 | 10.89 | 268.50 |
| Quality kg | 9.85 | 4.85 | 50.76 |

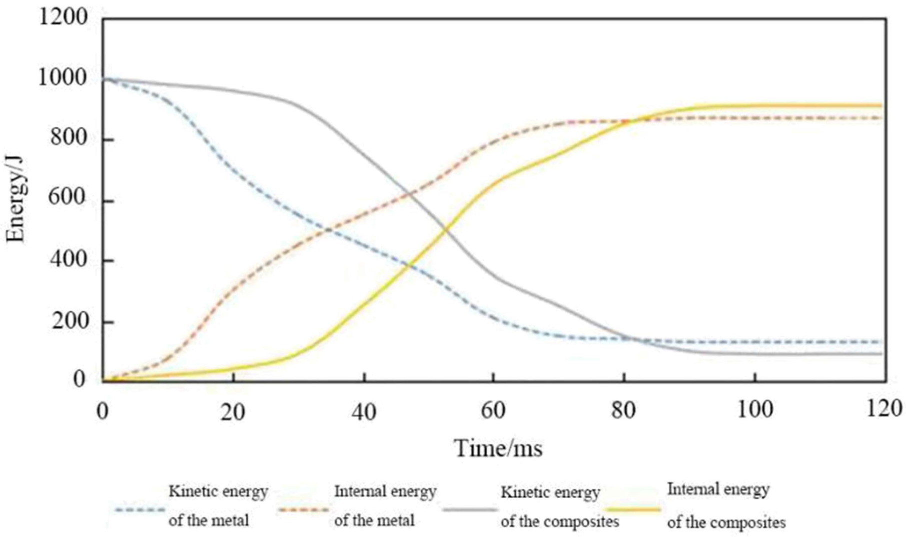


**Fig. 5.** Variations of kinetic energy and internal energy of two B-pillars during collision.

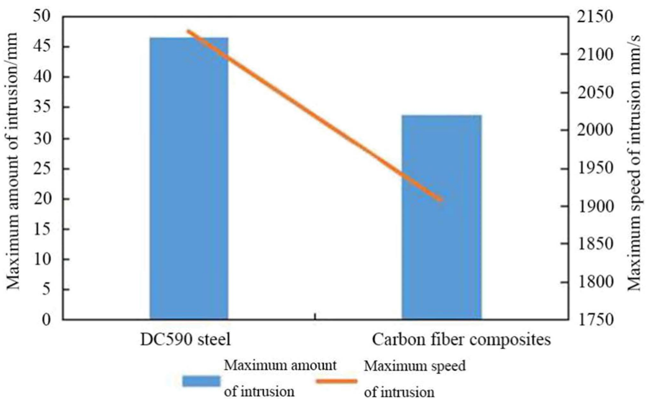


**Fig. 6.** The maximum amount of intrusion and the maximum speed of intrusion of the two B-pillars during collision.

The amount of intrusion is one of the metrics of the encroached internal safety space resulting from the deformation of the structure after the car is impacted. The excessive amount of intrusion leads to insufficient internal safety space, resulting in more collision damage to the passengers when the car collides and tumbles. The speed of intrusion is the metrics of the speed of structural deformation encroaching on the internal space after the car is impacted, and the deformation structure will have a great impact on passengers when the intrusion speed is too large. As shown in Fig. 6, the maximum amount of intrusion of the metal B-pillars is 46.60 mm, and the maximum speed of intrusion is 21297.76 mm/s; the maximum amount of intrusion of the carbon fiber composites B-pillars is 33.87 mm, and the maximum speed of intrusion is 1,905.53 mm/s. It can be seen from the comparison in Fig. 6 that the amount of intrusion and the speed of intrusion of the carbon fiber composites B-pillars are smaller, which are respectively reduced by 27.32 % and 10.48 %. The reason is that as a metal, the internal structure of DC590 steel has regular isotropy, which is easy to deform when impact occurs. As shown in Fig. 6, the carbon fiber composites have an anisotropic structure in the fiber part, and moreover the matrix is strengthened. When impact occurs, the impact will be buffered by the fracture of the matrix and fiber. Therefore, compared with the metal B-pillars, the carbon fiber composites B-pillars has better capability of elastic deformation and impact resistance.

## 5. Conclusion

In this paper, the carbon fiber composites and the automobile B-pillars are briefly introduced, and then the mechanical properties and impact resistance of the DC590 steel B-pillars and carbon fiber composites B-pillars are simulated by the ABAQUS finite element software. The composites B-pillars are obtained by the replacement material of metal B-pillars according to the principle of equal stiffness approximation. Through the experiment, the mass of the carbon fiber composites B-pillars is reduced by 50.76 % under the same size specification, and the stiffness, ultimate load of tensile, cantilever bending and fixed-branch bending of carbon fiber composites B-pillars of unit mass are significantly higher than that of metal B-pillars. In the process of collision, the impact resistance of the composites B-pillars is higher in the aspect of the comparison of conversion of kinetic energy and internal energy and the comparison of the amount and speed of intrusion. In summary, carbon fiber composites can effectively reduce the weight of automobiles under the premise of improving impact resistance.

## References


1. H. Cheng, H. Xue, C. Hong and X. Zhang, Compos. Sci. Technol., **140**, 63 (2017).
2. J. G. Cho, J. S. Koo and H. S. Jung, J. Mech. Sci. Technol., **30**, 673 (2016).
3. P. Vitale, G. Francucci, H. Rapp and A. Stocchi, Compos. Struct., **194**, 188 (2018).
4. B. Xu, S. Zhou, C. Hong, J. Han and X. Zhang, Carbon, **102**, 487 (2016).
5. Z. Liu, J. Lu and P. Zhu, Compos. Struct., **140**, 630 (2016).
6. D. H. Kim, H. G. Kim and H. S. Kim, Compos. Struct., **131**, 742 (2015).
7. Y. Hu, C. Liu, J. Zhang, G. Ding and Q. Wu, Adv. Mech. Eng., **7**, 1 (2015).
8. M. Hengstermann, N. Raithel, A. Abdkader and C. Cherif, Mater. Sci. Forum, **825-826**, 695 (2015).
9. H. D. Nguyen-Tran, V. T. Hoang, V. T. Do, D. M. Chun and Y. J. Yum, Materials, **11**, 429 (2018).
10. B. Xu, R. He, C. Hong, Y. Ma, W. Wen, H. Li, T. Cheng, D. Fang, Y. Yang, J. Alloy. Compd., **702**, 551 (2017).
11. Z. Zhe and D. Yu, Appl. Acoustics, **120**, 34 (2017).
12. J. Kaufmann, H. Rabe, N. Siebert, P. Wolf, H. Cebulla and S. Odenwald, Proc. Eng., **147**, 562 (2016).
13. Q. Luca, D. Kim, C. Jang, N. Kim and S. Hong, Fract. Fatigue Wear, (2017) p. 012017.
14. H. Y. Li, Y. Dai, X. F. Lyu, Mater. Sci. Forum, **921**, 85 (2018).
15. I. S. Son, Y. J. Shin, J. B. Park, G. P. Son, D. K. Shin and J. J. Lee, Appl. Mech. Mater. **749**, 286 (2015).